MOLECULAR DYNAMICS STUDY OF THE STRUCTURAL ROLE OF METAL ATOMS IN THE UREASE ACTIVE SITE

Lisnyak Yu. V., Martynov A. V.

Mechnikov Institute of Microbiology and Immunology

Introduction

Urease is a representative of a small group of enzymes that can bind different alternative metals to execute the same catalytic function. The presence of nickel as a metal cofactor in urease intrigued the scientific community since its discovery [1]. To check the possibility of catalysis by a urease containing other alternative metals, in the *Klebsiella aerogenes* urease Ni(II) ions were substituted by ions Zn(II), Co(II), Cu(II) and Mn(II) [2]. All of these urease derivatives, except Mn(II)-urease, were inactive, and in the case of Mn(II)-derivative activity was at the level of 0.3% relative to Ni(II)-urease. In the crystal state of *K. aerogenes* urease, the structures of the active site in Mn(II)- and Ni(II)-derivatives were very similar. An analogous situation was observed in the case of Fe(II)-containing *Helicobacter mustelae* urease. *Helicobacter mustelae*, a gastric pathogen of ferrets, synthesizes an iron-dependent urease in addition to its archetypical Ni(II)-containing urease [3]. The researchers conclude that a urease activity critically depends on the precise positions of amino acid ligands at a metallocenter, the bound solvent molecules and the type of metal [2], and very subtle changes of metallocenter structure can essentially influence the urease activity. These conclusions were based on the comparisons of urease derivatives structures in the crystal state. Are these conclusions valid in the case of the urease structures in the solution? By molecular dynamics simulations, we studied these aspects for urease derivatives with alternative metals in solution under physiological pH and temperatures.

Methods

The coordinates of ureases structures used in the simulations (Table 1) were retrieved from Protein Data Bank [4]. To reduce computation time we considered only α subunits that contain a urease active site. The systems studied (α subunits or its complex with competitive inhibitor) were placed in a cubic periodic cell filled with TIP3P water molecules. The simulation cell was 1 nm larger than the molecular system studied along all three axes. Na^+ and Cl^- counterions were added to neutralize the system and to reach ion mass fraction 0.9% NaCl. Before simulations the systems were energy-minimized. After a short steepest descent minimization, the

Table 1 – Urease structures used in the simulations.

Source	PDB code	Resolution	Description	References
Sporosarcina pasteurii	4ubp	1.55 Å	Ni-containing urease inhibited with AHA	[5]
Sporosarcina pasteurii	2ubp	2.0 Å	Ni-containing urease	[6]
Klebsiella aerogenes	1fwj	2.2 Å	Ni-containing urease	[7]
Klebsiella aerogenes	1ef2	2.5 Å	Mn-containing urease	[2]
Helicobacter mustelae	3qga	3.0 Å	Fe-containing urease	[3]

the procedure continued by simulated annealing minimization. AMBER14ipq force field was used [8]. To treat long-range electrostatic interactions the Particle Mesh Ewald algorithm [9] was used. The equations of the movement were integrated by 2.5 fs step. To speed up the calculations the non-bounded van der Waals and electrostatic forces were evaluated only each second step and added with the scaling factor 2 [10]. The molecular dynamics simulations were run in NPT ensemble at pH 7.4 and two temperatures (298 K and 310 K). Trajectories were computed for 50 ns, the data were saved each 25 ps. Models building, structure refinement, molecular dynamics simulations, and analysis as well as the result presentation by using molecular graphics were performed by using the molecular modeling program YASARA Structure [11-14]. Homology modeling of the *H. mustelae* urease mobile flap (lacking 329-332 amino acid residues in the original structure) was performed as described in [15].

Results and discussion

Global structure of the urease subunit α. Molecular dynamics (MD) simulations were carried out for the following systems: Ni-containing *Sporosarcina pasteurii* urease both native (PDB code 2ubp) and in complex with competitive inhibitor acetohydroxamic acid, AHA (PDB code 4ubp); *Klebsiella aerogenes* urease both Ni- and Mn-containing (PDB codes 1fwj and 1ef2, respectively); Fe-containing *Helicobacter mustelae* urease (PDB code 3qga) (table 1). As well, there was studied an apoenzyme of Ni-containing urease: the structure of the complex of competitive inhibitor AHA with *Sporosarcina pasteurii* urease (4ubp) from which there were removed Ni atoms.

DOI: 10.5281/zenodo.3726649

During the simulation, root mean square deviations (RMSD) of the enzyme's backbone atoms were monitored. As can be seen from fig.1, after equilibration (beyond 20 ns) RMSD values for different systems are close to each other and change insignificantly (except Fe-containing *Helicobacter mustelae* urease), evidencing that their global structure is quite stable and that no significant

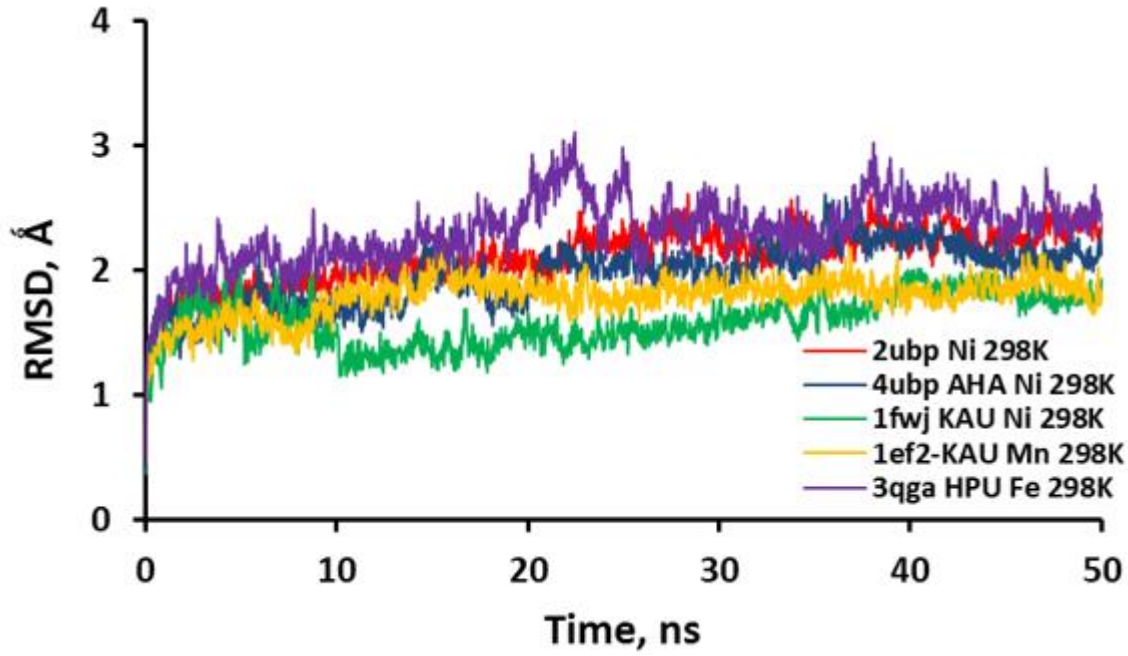

Fig. 1 – Time evolution of the backbone root mean square deviation (RMSD) at 298 K.

conformational transformations occur within these systems, whereas *H. mustelae* urease structure revealed instability during the simulations. Analogous stability of global structure was observed in the simulations at 310 K for all enzymes, except Fe-containing *H. mustelae* urease as well. In the latter case, RMSD values were essentially higher than ones for other ureases (fig.2). These deviations can be explained by the low resolution of the original experimental *H. mustelae* urease structure (table 1) and by the fact that the structure lacks 329-332 amino acid residues of the mobile flap (we determined their positions by homology modeling). As a result, during the optimization and further molecular dynamics simulations of the enzyme structure the significant artifact conformational changes occurred which did not allow us to study correctly the properties of the active site of this urease.

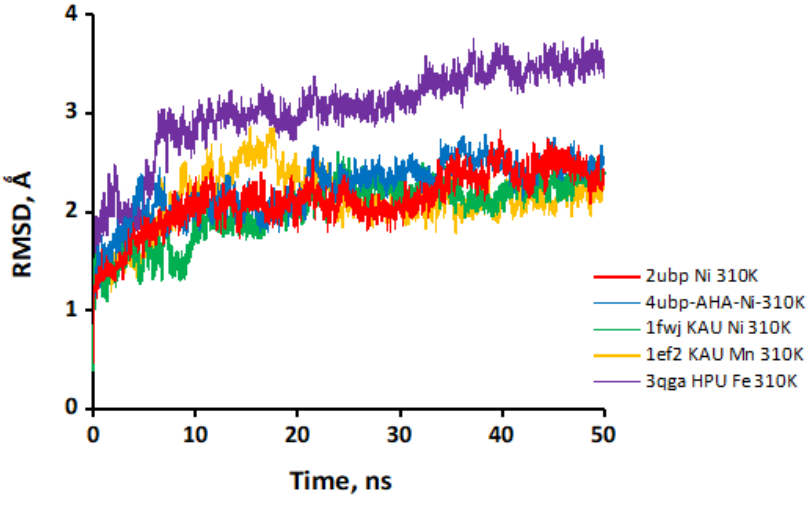

Fig. 2 – Time evolution of the backbone root mean square deviation (RMSD) at 310 K.

DOI: 10.5281/zenodo.3726649

Structure of the active site of the urease holoenzyme. The active site of the Ni-ureases contains two Ni^{2+} ions bridged by two oxygen atoms of a carbamylated lysine residue. Each of the two Ni^{2+} ions is bounded to two histidines, and one nickel ion is additionally bounded to the aspartic acid. Each of the two Ni^{2+} ions is bonded to a water molecule (W1 or W2) and hydroxyl-ion (Wb) (fig. 3). As a result, ion Ni1 is five-coordinated with deformed square-pyramidal geometry, and Ni2 ion is six-coordinated with deformed octahedral geometry [16] (fig. 3). Water molecules W1 and W2 along with the hydroxyl-ion Wb and additional water molecule W3 form close to Ni^{2+} ions tetrahedral cluster which is similar to the substrate urea by its size and shape [16].

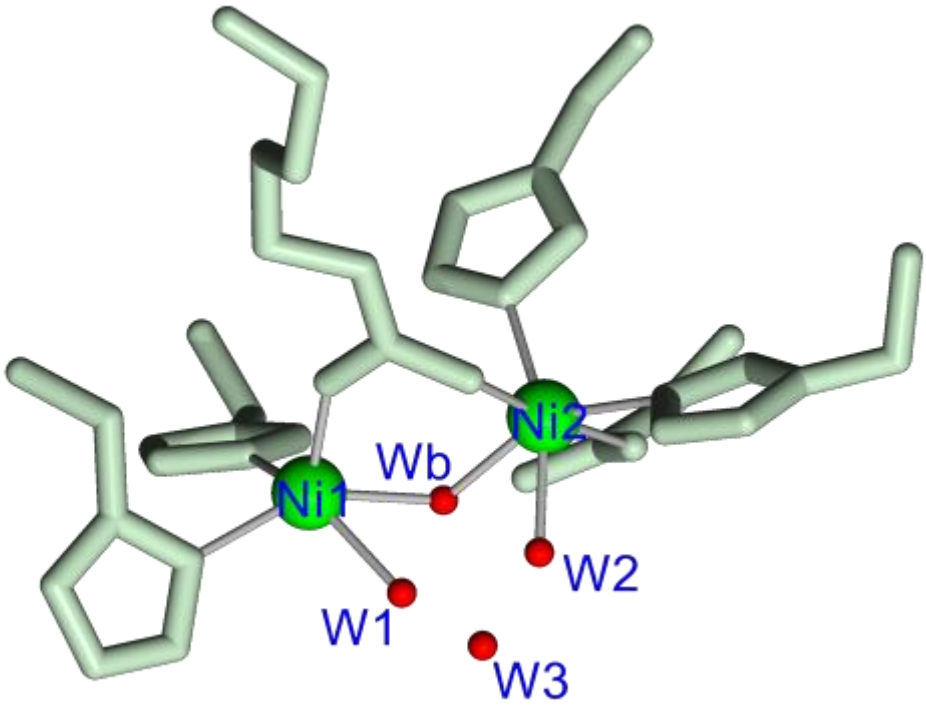

Fig. 3 – Active site of *S. pasteurii* urease (2ubp). Hydrogen atoms are not shown. Nickel ions are green colored, oxygen atoms of water molecules W1-W3 and hydroxyl ion are colored in red.

By low-temperature measurements of magnetic susceptibility of the jack bean urease and its complex with competitive inhibitor acetohydroxamic acid (AHA), P. A. Clark and D. E. Wilcox showed that the binding of the urease with the competitive inhibitor induces the significant increase of the urease magnetic moment that may indicate the change of the coordination number and/or the geometry of binding of the ion/ions with the active site ligands at the binding of the competitive inhibitor [17]. Does the competitive inhibitor induce any changes in the metal ion coordination number? What are the changes in the active site geometry (if they exist) near the metal ions? Does the temperature effect the metal ion coordination and the active site geometry near the metal ions? We studied these aspects by molecular dynamics simulations at two different temperatures.

Effect of the competitive inhibitor on the active site structure of the urease holoenzyme. By an analysis of the trajectories of molecular dynamics, there were determined average structures of the ureases studied. To investigate the effect of the competitive inhibitor on the active site structure of the urease holoenzyme, we have compared the active sites of the average structures of the native *S. pasteurii* urease (2ubp) and its complex with the competitive inhibitor AHA (4ubp). As can be seen from Table 2, the presence of the competitive inhibitor in the active site did not change the Ni (1) and Ni (2) coordination numbers. There were observed no essential deformations of the geometry of the ions binding with the active site ligands as well (fig. 4). A similar situation was observed in the case of Mn-containing *K. aerogenes* urease (1ef2) too (Table 2). The calculated average distances between the Ni ions and the ligands (both the amino acid residues, and the competitive inhibitor) agrees well with the data of experimental studies of the structure of these ureases (Table 3). Especially it concerns the *S. pasteurii* urease

DOI: 10.5281/zenodo.3726649

structure (4ubp). Also, we studied the geometry of metal ions binding with water molecules and hydroxyl-ion during the molecular dynamics simulations (Table 4).

The calculated average "metal-water" distances were a little bit shorter than experimental ones whereas the calculated average "water-water" distances, in the opposite, were a little bit longer than experimental ones. In the case of Ni-containing *K. aerogenes* urease (fig. 5), as can be seen from the time evolution of the root mean square deviation (RMSD) of the positions of the hydroxyl ion W725 and the water

Table 2 – Metal coordination bonds in the urease active site.

Metal	Coordi-nation number	Ligands	Origin	PDB code
Ni (1)	5	Lys 220, His 249, His 275, WB 990, W1 972	*S. pasteurii*	2ubp
Ni (2)	6	His 137, His 139, Lys 220, Asp 263, WB 990, W2 1043		
Ni (1)	5	Lys 220, His 249, His 275, WB 990, W1 972	*S. pasteurii*	4ubp
Ni (2)	6	His 137, His 139, Lys 220, Asp 263, WB 990, W2 1043		
Mn (1)	5	Lys 217, His 246, His 272, W 500, W 501	*K. aerogenes*	1ef2
Mn (2)	6	His 134, His 136, Lys 217, Asp 360, W 500, W 502		

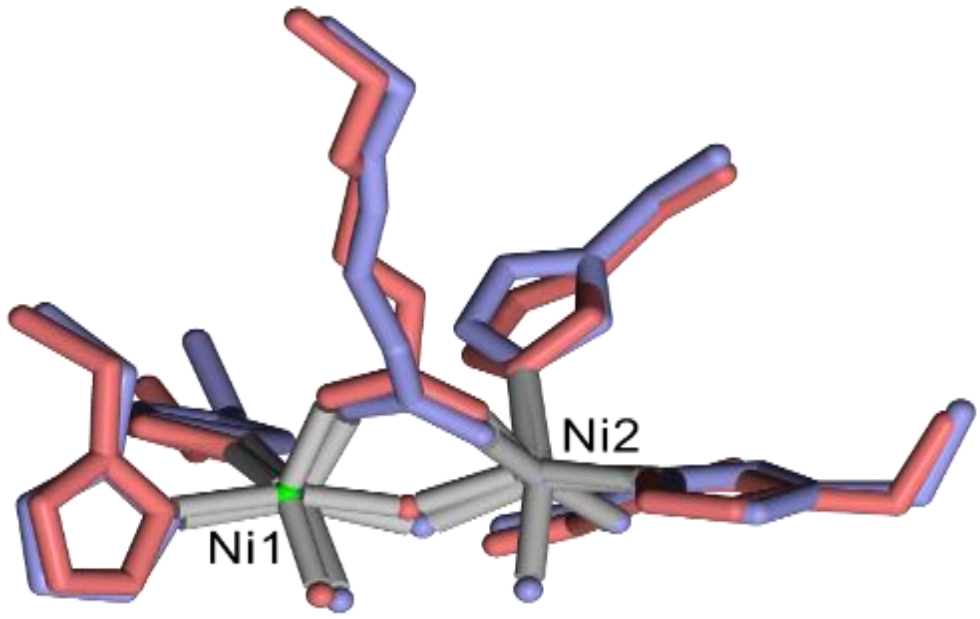

Fig. 4 – Superposition of the average active site structures of the native *S. pasteurii* urease (2ubp, light-blue colored) and its complex with AHA (4ubp, pink-colored). Ni ions are green colored. The Ni ions coordination bonds are colored in grey

molecules W726 and W727 (fig. 6), the position of this water cluster near the Ni ions and the geometry of its binding with the nickel ions do not change practically during the MD simulations. Similarly, in the case of Mn-containing *K. aerogenes* urease (fig. 7) after equilibration, RMSD values for hydroxyl ion W500 are insignificant (fig. 8). The RMSDs for water molecules W501 and W502 after equilibration are slightly higher compared to the Ni-containing urease but again they insignificantly oscillate near their low average values.

Thus, according to our results, the binding of the competitive inhibitor does not change the metal ion coordination in the active site of the urease holoenzyme and does not significantly affect the geometry of the active site near the metal ions.

The active site structure of the urease apoenzyme. To investigate the role of the Ni ions in the urease active site

DOI: 10.5281/zenodo.3726649

we carried out the molecular dynamics simulations of the *S. pasteurii* urease complex with the competitive inhibitor AHA in the presence and the absence of Ni ions in the active site and compared the structural features of these systems. In the latter case, we used the experimental structure 4ubp from which there were deleted the Ni ions. E. Jabri and P.A. Karplus in the frame of their investigation of structure-function relations of the *K. aerogenes* urease by X-ray analysis studied the structure of the *K. aerogenes* urease apoenzyme [19]. They showed that its structure is approximately identical to one of the apoenzyme. In the apoenzyme, all residues-ligands of Ni ions are shifted from their positions less than 0.5 Å compared to ones in the holoenzyme.

Prerequisite of such stability of the active site supposed to be the high degree of pre-organization of the urease structure that explains the tight interactions of Ni ions with the active site ligands [19].

Fig. 5 – Active center of Ni-containing *K. aerogenes* (1fwj) urease. Hydrogen atoms are not shown. Nickel ions are green-colored, oxygen atoms of the hydroxyl ion W725 and the water molecules W726 and W727 are colored in red.

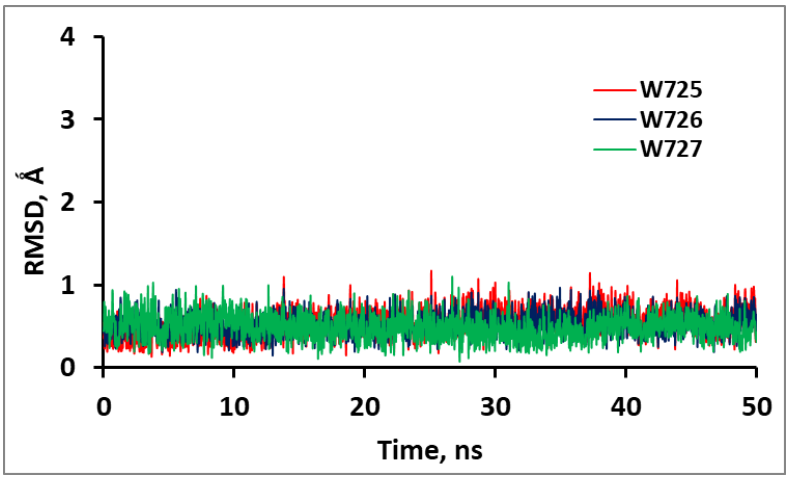

Fig. 6 – Time evolution of the root mean square deviation (RMSD) of the positions of the hydroxyl ion W725 and the water molecules W726 and W727 in the active site of *K. aerogenes* urease (1fwj) at 298 K.

Fig. 7 – Active site of Mn-containing *K. aerogenes* (1ef2) urease. Hydrogen atoms are not shown. Mn ions are yellow-colored, their coordination bonds are colored in gray. Amino acid residues and oxygen atoms of the hydroxyl ion W500 and the water molecules W501 and W502 are pink-colored.

DOI: 10.5281/zenodo.3726649

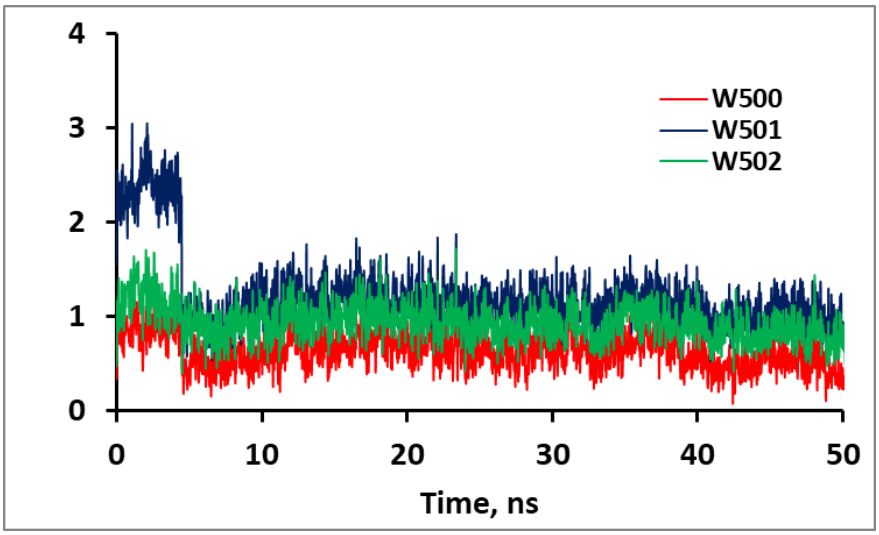

Fig. 8 – Time evolution of the root mean square deviation (RMSD) of the positions of the hydroxyl ion W500 and the water molecules W501 and W502 in the active site of *K. aerogenes* urease (1ef2) at 298 K.

According to our simulations, in the case of *S. pasteurii* urease apoenzyme, there were observed the insignificant shifts of the active site residues as well (fig. 9).

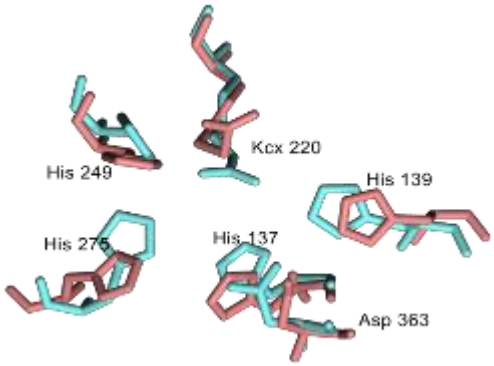

Fig. 9 – Superposition of the active site residues in the average structures of the complex of *S. pasteurii* urease with the competitive inhibitor in the presence (aquamarine-colored) and absence of Ni ions (magenta-colored).

DOI: 10.5281/zenodo.3726649

Table 3 - Metal (Me)-ligand (L) distances (in Å) in the urease active site [(a)].

Me1…Me2	3.53	3.65	3.58	3.56	3.70	3.54	3.53	3.44	3.22	2.87	3.59	3.13	3.13
His249 Nδ…Me1	1.96	2.41	2.03	2.03	2.20	2.20	2.21	2.17	2.22	2.23	2.03	2.02	2.02
His275 Nε…Me1	2.03	2.14	2.06	2.05	2.16	2.18	2.18	2.60	2.61	2.61	2.28	2.31	2.30
Lys220 Oθ1…Me1	1.95	1.95	1.96	1.96	2.08	2.04	2.04	2.18	2.16	2.19	2.08	2.02	2.02
AHA OB…Me1	1.95	1.99	1.98	1.98	-	-	-	-	-	-	-	-	-
AHA OT…Me1	2.15	1.97	1.96	1.95	-	-	-	-	-	-	-	-	-
His137 Nε…Me2	1.99	2.18	2.02	2.03	2.23	2.22	2.22	2.63	2.61	2.61	2.26	2.21	2.22
His139 Nε…Me2	1.99	2.19	2.04	2.03	2.20	2.19	2.19	2.33	2.32	2.32	2.15	2.16	2.16
Lys220 Oθ2…Me2	2.04	1.96	2.01	2.01	2.10	2.06	2.06	2.07	2.04	2.02	2.08	2.01	2.01
Asp363 Oδ1…Me2	2.07	1.96	2.00	2.00	2.21	2.18	2.17	2.39	2.37	2.36	2.18	2.18	2.18
AHA OB…Me2	2.01	2.01	1.97	1.96	-	-	-	-	-	-	-	-	-
Metal (Me1…Me2)	Ni-Ni	Ni-Ni	Ni-Ni	Ni-Ni	Ni-Ni	Ni-Ni	Ni-Ni	Mn-Mn	Mn-Mn	Mn-Mn	Ni-Ni	Ni-Ni	Ni-Ni
Temperature, K	100K	300K	298K	310K	100K	298K	310K	298K	298K	310K	298K	298K	310K
PDB code	4ubp[b]	4ubp[c]	4ubp[d]	4ubp[d]	2ubp[b]	2ubp[d]	2ubp[d]	1ef2[b]	1ef2[d]	1ef2[d]	1fwj[b]	1fwj[d]	1fwj[d]
Source[e]	Spu	Spu	Spu	Spu	Spu	Spu	Spu	Kau	Kau	Kau	Kau	Kau	Kau

[a] – Residue numbering from *S. pasteurii* is used; [(b)] – experimental X-ray data (see refs in Table 1); [(c)] – MD data from ref. 18;
[d] –MD data from our simulations; [e] – Spu - *S. pasteurii* urease, Kau - *K. aerogenes* urease.

DOI: 10.5281/zenodo.3726649

Table 4 - Metal-water distances (in Å) in the urease active site.

Me1-W1	2.15	2.01	2.01	2.17	2.12	2.09	2.11	1.95	1.96
Me2-W1	1.98	1.71	1.71	2.23	2.10	2.08	2.17	2.06	2.06
Me2-W3	2.13	1.97	1.97	2.45	2.44	2.42	2.11	1.98	1.98
Me1-W2	2.09	1.78	1.78	2.84	1.94	2.20	2.18	2.13	2.13
W1-W2	2.49	2.46	2.45	1.98	2.75	3.64	2.09	2.45	2.44
W1-W3	2.02	2.36	2.35	1.93	2.34	2.37	2.24	2.38	2.39
W2-W3	2.26	2.59	2.61	1.81	2.86	2.60	2.14	2.79	2.72
Metal	Ni	Ni	Ni	Mn	Mn	Mn	Ni	Ni	Ni
W1	Wb	Wb	Wb	W725	W725	W725	W500	W500	W500
W2	W1	W1	W1	W726	W726	W726	W501	W501	W501
W3	W2	W2	W2	W727	W727	W727	W502	W502	W502
Temperature, K	298	298	310	298	298	310	100	298	310
PDB code	1fwj [a]	1fwj	1fwj	1ef2 [a]	1ef2	1ef2	2ubp [a]	2ubp	2ubp
Source [b]	Kau	Kau	Kau	Kau	Kau	Kau	Spu	Spu	Spu

[a] – Experimental X-ray data (see refs in Table 1); [b] – Spu - *S. pasteurii* urease, Kau - *K. aerogenes* urease

DOI: 10.5281/zenodo.3726649

.

The root mean square deviation of the residues of the active site of apoenzyme relative to holoenzyme was 0.65 Å. Our results are compatible with the calculation data of J. Lv et al. [18]: the root mean square deviation of the residues of the active site of the *S. pasteurii* urease holoenzyme and apoenzyme were 0.38 Å and 1.02 Å, correspondingly.

In the absence of Ni ions in apoenzyme, the position of the inhibitor AHA within the active site is unstable: the AHA molecule gradually drifts and leaves the active site (fig. 10). Such behavior of the inhibitor may denote that the main factors of the inhibitor (or substrate) binding are the Ni ions, and the main driving forces of binding are its electrostatic interactions with Ni ions, whereas the active site residues compose the substrate recognition site only [18].

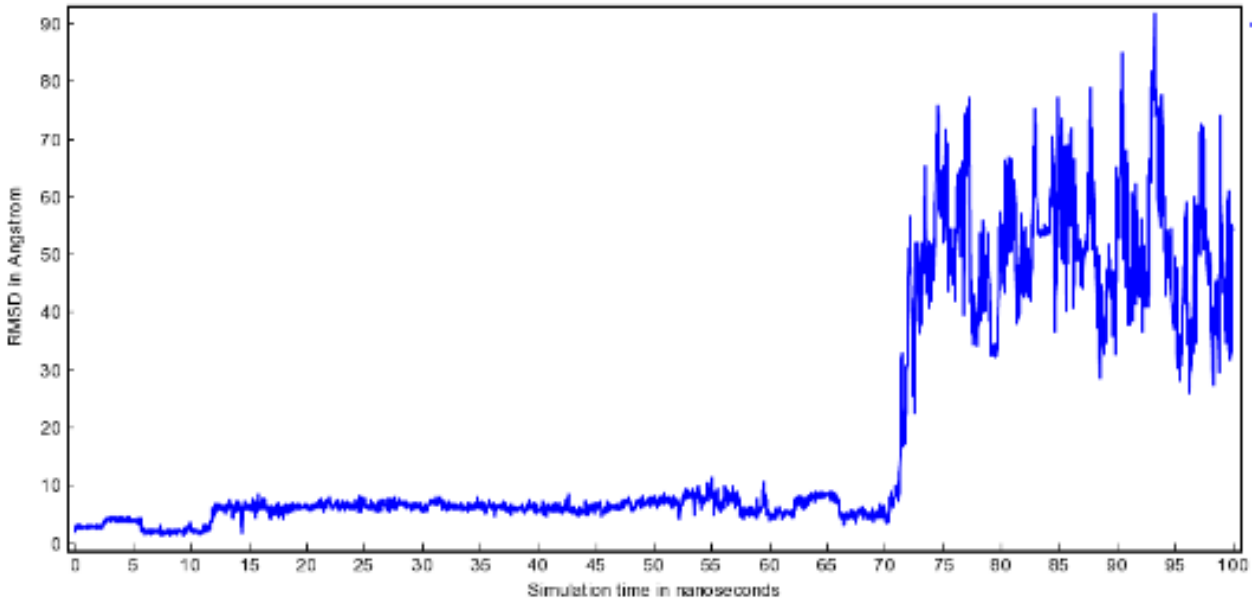

Fig. 10 – The hydroxamic acid (AHA) movement RMSD after superposing on the receptor structure as a function of simulation time.

The temperature effect on the urease active site structure. For all ureases, the temperature increase from 298 K to 310 K had a little effect on the average distances "metal-ligand". The calculated average distances "metal-ligand" reproduced the corresponding experimental values better than the average distances "metal-metal". The latter were shorter than experimental ones. In the case of Mn-containing urease, the calculated average distances were, in general, longer than the analogues values for the Ni-containing *K. aerogenes* urease and they were very similar to the experimental ones both at 298 K and 310 K, except Mn-Mn distance that similar to Ni-containing urease was shorter than the experimental one. The temperature increase did not change the Ni-Ni distances, but in the case of Mn-containing urease, the increase of temperature resulted in the shortening of the Mn-Mn distances (Table 3).

The temperature increase from 298 K to 310 K had an insignificant effect on the distances "metal-water" in the active site of the Ni-containing ureases *S. pasteurii* (2ubp) and *K. aerogenes* (1fwj) and a little influence on these distances in the Mn-containing *K. aerogenes* urease (1ef2) (see Table 4).

As can be seen from the time evolution of the root mean square deviation of the positions of the hydroxyl ion W725 and the water molecules W726 and W727 in the active site of Ni-containing *K. aerogenes* urease at 310 K (fig. 11), the position of the molecules of this cluster near Ni ions and the geometry of their binding with

DOI: 10.5281/zenodo.3726649

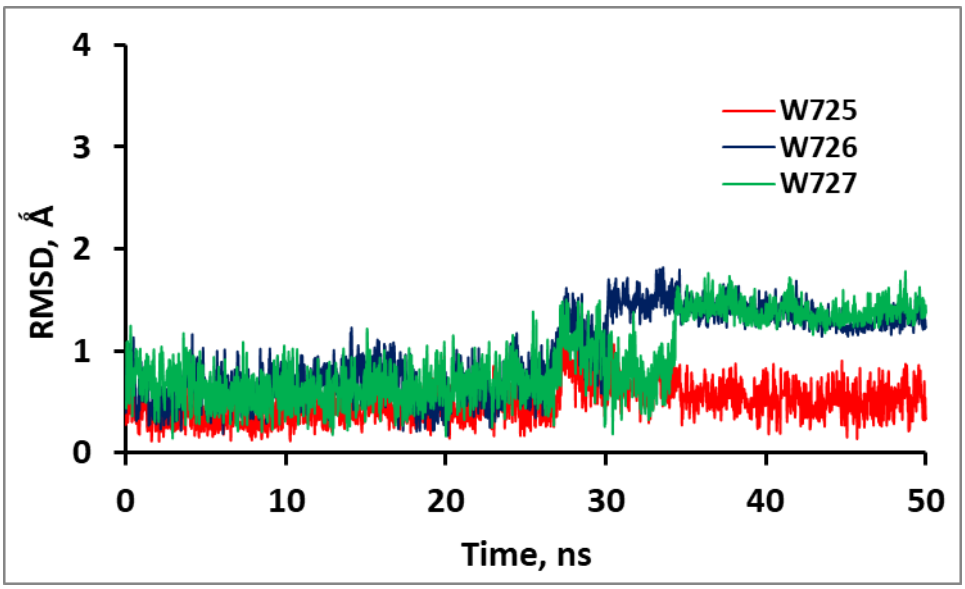

Fig. 11 – Time evolution of the root mean square deviation (RMSD) of the positions of the hydroxyl ion W725 and the water molecules W726 and W727 in the active site of *K. aerogenes* urease (1fwj) at 310 K.

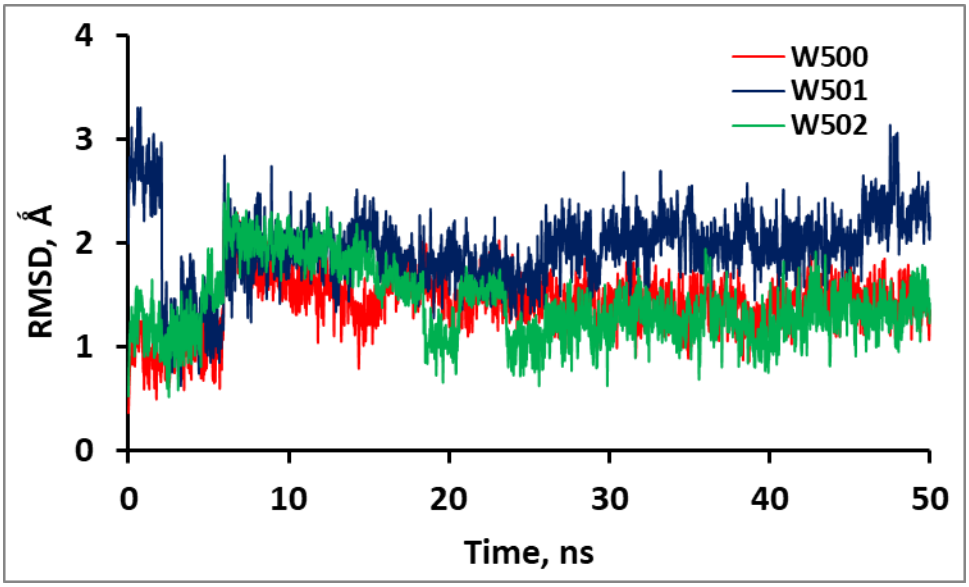

Fig. 12 – Time evolution of the root mean square deviation (RMSD) of the positions of the hydroxyl ion W500 and the water molecules W501 and W502 in the active site of *K. aerogenes* urease (1ef2) at 310 K.

the Ni ions are practically unchanged until approximately 27 ns and then the water molecules W726 and W727 noticeably moved from their original positions whereas hydroxyl-ion W725 saved its position.

In the case of Mn-containing *K. aerogenes* urease, the water molecules and hydroxyl-ion after equilibration at 310 K are more shifted from their initial positions (fig. 12) compared to the situation at 298 K (fig. 8). The average RMSD are near 1.5 Å for the hydroxyl-ion W500 and water molecule W502, and near 2.0 Å for water molecule W501 (fig. 12). But their distances to metal ion changed by no more than 0.3 Å (Table 4), and overall structure of the water cluster and its interactions with metal ions remained stable.

The effect of cation type on the urease active site structure. The average Mn-Mn metallocentre structure of *K. aerogenes*

DOI: 10.5281/zenodo.3726649

urease is very close to the average metallocentre structure of Ni-containing *K. aerogenes* urease (fig.13).

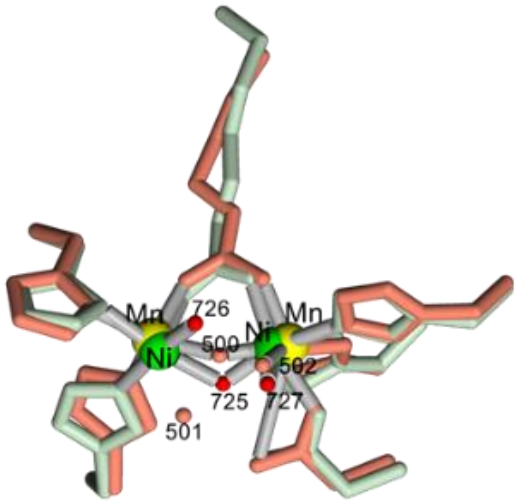

Fig. 13 – Superposition of the average active site structures of the Ni- and Mn-containing *K. aerogenes* ureases (1fwj i 1ef2, correspondingly). In the first structure, the Ni ions are colored in green, the residues and the coordination bonds are grey-colored, and the oxygen atoms of the hydroxyl ion W725 and the water molecules W726 and W727 are colored in red. In the second structure, the Mn ions are colored in yellow, the coordination bonds are gray-colored, the residues and the oxygen atoms of the hydroxyl ion W500 and the water molecules W501 and W502 are colored in pink.

The average distances Mn-Mn and Ni-Ni are 3.22 Å and 3.13 Å, respectively (Table 3). In Mn-urease, the root mean square deviation of the positions of ligands His 134, His 136, His 246, His 272, Asp 360 and carbamylated Lys 217 from ones of the corresponding ligands in Ni-urease structure is 0.57 Å (fig. 13). Three water molecules are shifted from the metal (at least partially due to the larger size of Mn compared to Ni): W500 by 0.1 Å, W501 by 0.4 Å and W502 by 0.5 Å. Due to these shifts of the water molecules, the distances "metal-water" in Mn-urease are 1.94÷2.44 Å compared to 1.71÷2.01 Å in Ni-urease. These distances in the corresponding crystal structures are within 2.17÷2.84 Å and 1.98÷2.15 Å, respectively (Table 4). Thus, the metallocentre structures in the Mn- and Ni-containing *K. aerogenes* ureases are very similar.

Conclusions

The structural role of the nickel ions in a urease active site, the influence of the temperature and the ion type on the structure of the urease active site have been stusied by molecular dynamics simulations. It have been shown that binding of the competitive inhibitor (acetohydroxamic acid, AHA) did not change the Ni ions coordination in the urease active site and did not essentially effect the geometry of the active site near the nickel ions. The main factor of the inhibitor binding are the nickel ions. It have been shown that the active site structures of the Ni- and Mn-containing ureases *Klebsiella aerogenes* and *Sporosarcina pasteurii* are approximately identical. It have been shown that the metallocentre structure of these ureases are in general stable regardless of the urease source, the ion type and the temperature.

References

1. Maroney M. J., Ciurli S. Nonredox nickel enzymes. Chem. Rev. 2014. Vol. 114, N 8. P. 4206-4228.
2. Yamaguchi K., Cosper N. J., Stalhandske C., Scott R. A., Pearson M. A., Karplus P. A., Hausinger R.P Characterization of metal-substituted *Klebsiella aerogenes* urease. J.Biol.Inorg.Chem. 1999. Vol. 4. P. 468-477.
3. Carter E. L., Tronrud D. E., Taber S. R., Karplus P. A., Hausinger R. P. Iron-containing urease in a pathogenic bacterium. P. Natl. Acad. Sci. USA. 2011. Vol. 108. P. 13095-13099.
4. Protein Data Bank [Electronic resource]. – Mode of access: http://www.rcsb.org/pdb/home/home.do
5. Benini S., Rypniewski W. R., Wilson K. S., Miletti S., Ciurli S., Mangani S. The complex of *Bacillus pasteurii* urease with acetohydroxamate anion from X-ray data at 1.55 A resolution. J.Biol.Inorg.Chem. 2000. Vol. 5. P. 110-118.
6. Benini S., Rypniewski W. R., Wilson K. S., Miletti S., Ciurli S., Mangani S. A new proposal for urease mechanism based on the crystal structures of the native and inhibited enzyme from Bacillus pasteurii: why urea hydrolysis costs two nickels. Structure Fold.Des. 1999. Vol. 7. P. 205-216.

DOI: 10.5281/zenodo.3726649

7. Pearson M.A., Michel L. O., Hausinger R. P., Karplus P. A. Structures of Cys319 variants and acetohydroxamate-inhibited *Klebsiella aerogenes* urease. Biochemistry. 1997. Vol. 36. P. 8164-8172.
8. Cerutti D., Swope W., Rice J., Case D. ff14ipq: A self-consistent force field for condensed-phase. J.Chem.Theory Comput. 2014. Vol. 10, P. 4515-4534.
9. Essman U., Perera L., Berkowitz M. L., et al. A smooth particle mesh Ewald method. J. Chem. Phys. B. 1995. Vol. 103. P. 8577-8593.
10. Krieger E., Vriend G. New ways to boost molecular dynamics simulations. J.Comput.Chem. 2015. Vol.36. P. 996-1007.
11. Krieger E., Dunbrack R. L., Hooft R. W., Krieger B. Assignment of protonation states in proteins and ligands: combining pKa prediction with hydrogen bonding network optimization. Methods Mol. Biol. 2012. Vol. 819. P. 405-421.
12. Kreiger E., Joo , Lee J K., et al. Improving physical realism, stereochemistry, and side-chain accuracy in homology modeling: four approaches that performed well in CASP8. Proteins. 2009. Vol. 77, Suppl. 9. P. 114-122.
13. Krieger E., Darden T., Nabuurs S., et al. Making optimal use of empirical energy functions: force field parameterization in crystal space. Proteins. 2004. Vol. 57. P. 678-683.
14. Krieger E., Koraimann G., Vriend G. Increasing the precision of comparative models with YASARA NOVA - a self-parameterizing force field. Proteins. 2002. Vol. 47. P. 393-402.
15. Lisnyak Yu. V., Martynov A. V. Homology modeling and molecular dynamics study of *Mycobacterium tuberculosis* urease. Annals of Mechnikov Institute. 2017. N 3. P. 23-46.
16. Zambelli B., Musiani F., Benini S., Ciurli S. Chemistry of Ni^{2+} in urease: Sensing, trafficking, and catalysis. Accounts Chem. Res. 2011. Vol. 44. P. 520-530.
17. Clark P. A., Wilcox D. E. Magnetic properties of the nickel enzymes urease, nickel-substituted carboxypeptidase A, and nickel-substituted carbonic anhydrase Inorg. Chem. 1989. Vol. 28. P. 1326-1333.
18. Lv J., Jiang Y., Yu Q. Structural and functional role of nickel ions in urease by molecular dynamics simulation. J. Biol. Inorg. Chem. 2011. Vol. 16. P. 125-135.
19. Jabri E., Karplus P. A. Structures of the *Klebsiella aerogenes* urease apoenzyme and two active-site mutants. Biochemistry. 1996. Vol. 35. P. 10616-10626.

Molecular dynamics study of the structural role of metal atoms in the urease active site

Lisnyak Yu. V., Martynov A. V.

Introduction. Urease is a representative of a small group of enzymes that can bind different alternative metals to execute the same catalytic function. The experimental X-ray studies conclude that a urease activity critically depends on the precise positions of amino acid ligands at a metallocenter, the bound solvent molecules and the type of metal, and very subtle changes of metallocenter structure can essentially influence the urease activity. Are these conclusions valid in the case of the urease structures in the solution? By molecular dynamics simulations, we studied these aspects for urease derivatives with alternative metals in solution under physiological pH and temperatures. **Methods.** Molecular dynamics (MD) simulations were carried out for the following systems: Ni-containing *Sporosarcina pasteurii* urease both native (PDB code 2ubp) and in complex with competitive inhibitor acetohydroxamic acid, AHA (PDB code 4ubp); *Klebsiella aerogenes* urease both Ni- and Mn-containing (PDB codes 1fwj and 1ef2, respectively); Fe-containing *Helicobacter mustelae* urease (PDB code 3qga) (table 1). As well, there was studied an apoenzyme of Ni-containing urease: the structure of the complex of competitive inhibitor AHA with *Sporosarcina pasteurii* urease (4ubp) from which there were removed Ni atoms. The systems studied (α subunits or its complex with competitive inhibitor) were placed in a cubic periodic cell filled with TIP3P water molecules. The simulation cell was 1 nm larger than the molecular system studied along all three axes. Na^+ and Cl^- counterions were added to neutralize the system and to reach ion mass fraction 0.9% NaCl. Before simulations the systems were energy-minimized. After a short steepest descent minimization, the the procedure continued by simulated annealing minimization. AMBER14ipq force field was used. To treat long-range electrostatic interactions the Particle Mesh Ewald algorithm was used. The equations of the movement were integrated by 2.5 fs step. To speed up the calculations the non-bounded van der Waals and electrostatic forces were evaluated only each second step and added with the scaling factor 2. The molecular dynamics simulations were run in NPT ensemble at pH 7.4 and two temperatures (298 K and 310 K). Trajectories were computed for 50 ns, the data were saved each 25 ps. Models building, structure refinement, molecular dynamics simulations, and analysis as well as the result presentation by using molecular graphics were performed by using the molecular modeling program YASARA Structure. **Results and discussion.** After equilibration the RMSD values for different systems are close to each other and change insignificantly (except Fe-containing *Helicobacter mustelae* urease), evidencing that their global structure is quite stable and that no significant conformational transformations occur within these systems, whereas *H. mustelae* urease structure revealed instability during the simulations. The presence of the competitive inhibitor in the active site did not change the Ni (1) and Ni (2) coordination numbers. There were observed no essential deformations of the geometry of the ions binding with the active site ligands as well. A similar situation was observed in the case of Mn-containing *K. aerogenes* urease too. In the case of *S. pasteurii* urease apoenzyme, there were observed the insignificant shifts of the active site residues. The root mean square deviation of the residues of the active site of apoenzyme relative to holoenzyme was 0.65 Å. In the absence of Ni ions in apoenzyme, the position of the inhibitor AHA within the active site is unstable and it

DOI: 10.5281/zenodo.3726649

gradually drifts and leaves the active site. For all ureases, the temperature increase from 298 K to 310 K had a little effect on the average distances “metal-ligand”. The temperature increase from 298 K to 310 K had an insignificant effect on the distances “metal-water” in the active site of the Ni-containing ureases *S. pasteurii* and *K. aerogenes* and a little influence on these distances in the Mn-containing *K. aerogenes* urease. The metallocentre structures in the Mn- and Ni-containing *K. aerogenes* ureases are very similar.
Conclusions. There have been studied the structural role of the nickel ions in a urease active site, the influence of the temperature and the ion type on the structure of the urease active site. It have been shown that binding of the competitive inhibitor (acetohydroxamic acid, AHA) did not change the Ni ions coordination in the urease active site and did not essentially effect the geometry of the active site near the nickel ions. The main factor of the inhibitor binding are the nickel ions. It have been shown that the active site structures of the Ni- and Mn-containing ureases *Klebsiella aerogenes* and *Sporosarcina pasteurii* are approximately identical. It have been shown that the metallocentre structure of these ureases are in general stable regardless of the urease source, the ion type and the temperature.
Keywords: urease metallocentre, Ni-, Mn- and Fe-containing urease, molecular dynamics.

DOI: 10.5281/zenodo.3726649